Measurement of Package Inductance and Capacitance Matrices

Brian Young and Aubrey K. Sparkman

Abstract— **A technique is presented for the measurement of resistance, inductance, conductance, and capacitance matrices of large pin count electronic packages. Circuit analysis of an assumed lumped model is used to define a measurement technique based on two sets of measurements on specially prepared samples. Formulas are derived for use with network analyzer measurements. Measurements and simulations on a 208-lead quad flat pack show that the method attains good accuracy for all but the small values of the conductance matrix.**

Index Terms—**Resistance, inductance, conductance, and capacitance matrices, pin count, quad flat pack, noise**

I. Introduction

A COMPREHENSIVE computer analysis of noise in a digital system would include all inductive, capacitive, and resistive effects including all coupling terms, and if the rise time was sufficiently small, then retardation [1] would also be needed. It has been shown [2] that in the case of the mutual inductances, neglecting them induces a large error in noise simulation. Generally, when full capacitance and inductance matrices are used in circuit simulation, the matrices are produced by simulation [2]–[10], for which there is no shortage of techniques, methods, programs, and commercial products. Conversely, there has been little development in the measurement of large and full inductance and capacitance matrices.

Methods for measuring inductance and capacitance matrices of multiconductor transmission lines have appeared in the literature. In a frequency domain technique [11], a straightforward measurement of voltages and currents on suitable open- and short-circuits is used to obtain the short-circuit impedance matrix and the open-circuit admittance matrix from which the per-unit-length line parameters can be calculated. The characterization bandwidth for digital applications with rise times near 1 ns reach 1 GHz, so this technique lacks extendibility to high-performance digital packaging because voltage and current measurements are not suited to high frequency measurements. In various time-domain techniques [12]–[14], measurements of pulse amplitudes and timing are used to calculate the per-unit-length parameters. The very small size of packages makes the application of time-domain techniques difficult.

A method for measuring the capacitance matrix based on two-terminal capacitance measurements has been presented [15]. Since the technique relies on selective shorting of leads to ground, the measurement process is slowed by the repeated configuration of the shorts. The paper presents no extension to the technique for inductance matrix measurement.

To address the shortcomings of the above techniques, this paper presents a frequency-domain technique based on equipment suitable for high-frequency characterizations. The measurement of capacitance and inductance matrices of packages has several inherent difficulties: instrumentation has either one or two ports compared to the tens to hundreds of leads on the packages; small lead dimensions make for difficult connection to the instrumentation; and, the small dimensions produce very small electrical effects for measurement. A huge variety of techniques have been developed to characterize single package leads, including time-domain methods [16]–[21], low-frequency frequency-domain methods [20]–[23], and high-frequency frequency-domain methods [10], [24]–[29]. In addition, measurement of mutual inductance with a two-port technique, which is similar to the technique presented here, has been developed [24] based on the one-port technique reported in [25]. Network analyzers in conjunction with miniaturized probes have been shown to address the above difficulties [24], [25], [29] with good success.

In this work, a technique is presented for using one- and two-port network analyzer measurements with miniature probes to obtain full inductance and capacitance matrices for packages over a broad bandwidth including high frequencies. The technique does not rely on variable placement of shorts or opens. A specific implementation utilizing a vector network analyzer is presented.

II. Formulation

The formulation is based on a circuit analysis of the package model shown in Fig. 1. Application of Kirchhoff's voltage law yields

$$\bar{V}^L - \bar{V}^R = (\mathbf{R} + j\omega\mathbf{L})\bar{I}^L \tag{1}$$

where $\mathbf{L}$ is the inductance matrix and $\mathbf{R}$ is the diagonal resistance matrix. Application of Kirchhoff's current law yields

$$\bar{I}^R + \bar{I}^L = (\mathbf{G} + j\omega\mathbf{C})\bar{V}^R \tag{2}$$

where $\mathbf{C}$ is the capacitance matrix and $\mathbf{G}$ is the conductance matrix.

The technique presented here is based on one- and two-port vector network analyzer measurements. The vector network analyzer has several advantages: two measurement ports,

Manuscript received November 18, 1994; revised August 1, 1995.
The authors are with Motorola, Austin, TX 78735 USA.
Publisher Item Identifier S 1070-9894(96)00005-9.

1070–9894/96$05.00 © 1996 IEEE

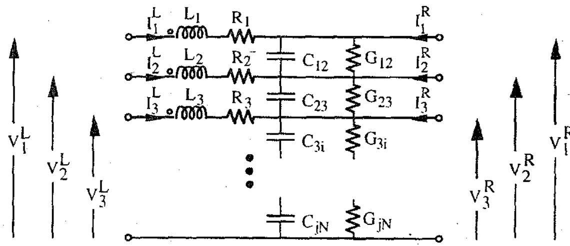

Fig. 1. Schematic of the package model. Note that most coupling terms are omitted in the figure for clarity.

high-frequency operation, and excellent compatibility with miniaturized high-frequency (microwave) probes. The probes are essential to achieve accurate measurement of very small quantities and high repeatability.

Since the general multiport S-parameters of the package are not the goal of the measurements, unused ports do not need to be terminated in the system impedance. For notational purposes, all measurements are assumed to take place on a one- or two-port device under test (DUT), and S-parameter notation for this DUT is used. Individual entries in matrices are indicated by a pair of subscripts. For an arbitrary matrix $\mathbf{A}$, the notation $\mathbf{A}_{ij}$ indicates the entry in row i at column j.

The equations describing the behavior of the package are given in (1) and (2). The need to consider them simultaneously can be avoided by selectively shorting lines to the reference or by leaving lines open-circuited. If $\bar{V}^R = 0$ is enforced with suitable shorts to the reference line, then (2) is automatically enforced, and (1) gives

$$\bar{V}^L = (\mathbf{R} + j\omega\mathbf{L})\bar{I}^L. \tag{3}$$

The characterization of (3) can be carried out in a two-step process consisting of one- and two-port measurements. For the one-port measurements, if just the mth line is driven and sensed by the network analyzer on port 1, then the currents on all other lines vanish, and the port 1 voltage relationship is

$$v_1 = (\mathbf{R} + j\omega\mathbf{L})_{mm} i_1. \tag{4}$$

Network analyzers measure the power of directional traveling waves. The total voltage can be written as $v_1 = V_1^+ + V_1^-$ and the total current can be written as $i_1 = \frac{1}{Z_0}(V_1^+ - V_1^-)$, where Z_0 is the system characteristic impedance (50 Ω typ). Plugging these into (4), and utilizing the relationship that $S_{11} = \frac{V^-}{V^+}$, then

$$(\mathbf{R} + j\omega\mathbf{L})_{\mathrm{mm}} = Z_0 \frac{1 + S_{11}}{1 - S_{11}}. \tag{5}$$

Therefore, the one-port measurements allow the diagonal terms to be measured.

In separate two-port measurements, if the mth line is sensed by port 1 and the nth line is driven by port 2, then all currents vanish except those on lines m and n, and the port 1 voltage relationship is

$$v_1 = (\mathbf{R} + j\omega\mathbf{L})_{\mathrm{mm}} i_i + (\mathbf{R} + j\omega\mathbf{L})_{\mathrm{mn}} i_2. \tag{6}$$

Substituting the traveling wave relationships into (6) and noting that $V_1^+ = 0$ due to the impedance match at port 1

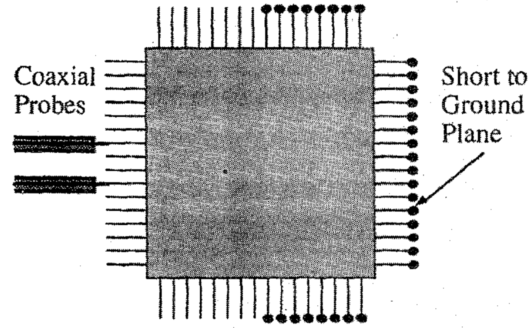

Fig. 2. Setup for two-port vector network analyzer measurements on a QFP. RL measurements use the shorts as shown, while GC measurements leave all leads open-circuited.

and that $S_{12} = \frac{V_1^-}{V_2^+}$, then

$$(\mathbf{R} + j\omega\mathbf{L})_{\mathrm{mn}} = [Z_0 + (\mathbf{R} + j\omega\mathbf{L})_{\mathrm{mm}}] \frac{S_{12}}{1 - S_{22}}. \tag{7}$$

Since $(\mathbf{R} + j\omega\mathbf{L})_{\mathrm{mm}}$ is known from prior one-port measurements, the two-port measurements allow the off-diagonal terms to be measured. The results from the one- and two-port measurements together fill out the entire resistance and inductance matrices.

For capacitance, (1) can be automatically satisfied $\bar{I}^L = 0$ if due to open circuits. Then (2) gives

$$\bar{V}^R = (\mathbf{G} + j\omega\mathbf{C})^{-1}\bar{I}^R \tag{8}$$

which is identical in form to (3). Therefore, the measurements and data reduction are given by (5) and (7) with the only difference that the inverse of $(\mathbf{G} + j\omega\mathbf{C})$ is filled out by the measurements. With the inverse matrix filled out, then $(\mathbf{G} + j\omega\mathbf{C})$ can be found by matrix inversion.

III. Measured and Simulated Results

The theory and techniques in the preceding section are demonstrated with two examples based on a 208-lead plastic quad flat pack (QFP). The QFP was prepared for experimental characterization in two configurations. In the first configuration, all of the leads are wirebonded to the flag, a setup tailor made to perform inductance and resistance measurements. In the second configuration, the leads are not wirebonded, so all leads are open-circuited for capacitance and conductance measurements. Both samples were fully molded, trimmed, and formed.

Both parts were mounted over a ground plane that serves as the reference. For GC measurements, all leads remain floating. For RL measurements, one half of the lead tips are shorted to the ground plane with pressure contacts while the remaining lead tips do not touch the ground plane. The setup is shown schematically in Fig. 2 and is based on a JEDEC proposal [32] for a standard setup. The measurement ports are defined between the lead tips and the ground plane, and coaxial probes make contact at these points.

The probing setup shown in Fig. 2 violates an implicit assumption regarding the location of the probes: it is assumed

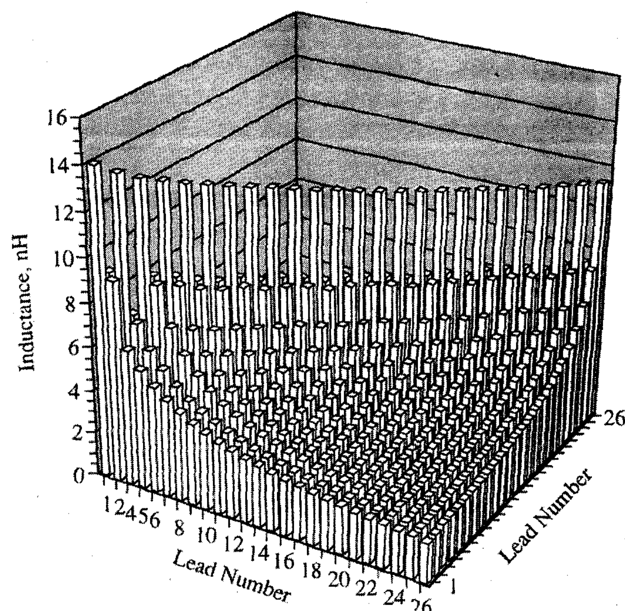

Fig. 3. Inductance matrix for 25 of 26 leads of a 208-lead QFP at 52 MHz.

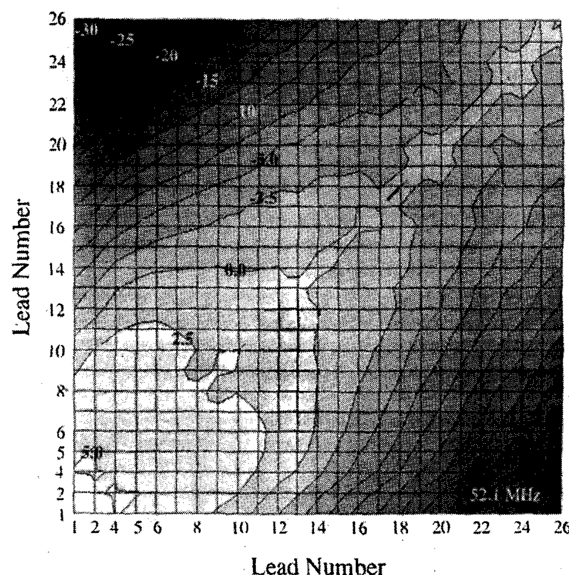

Fig. 4. Percent difference between simulation and measurement at 52.1 MHz using the measured data as base.

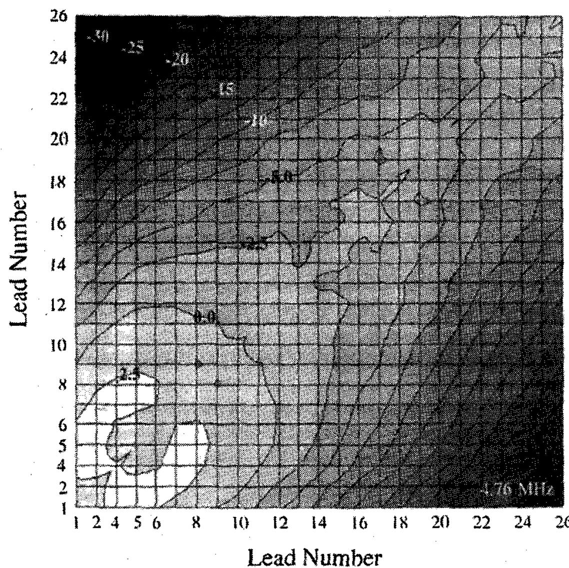

Fig. 5. Percent difference between simulation and measurement at 4.76 MHz using the measured data as base.

that the probe ground connects to the same point, which then becomes the reference, for every signal lead measured. In the setup in Fig. 2, the coaxial grounds contact different points, so a potential difference will exist. The error in the measurement introduced by this probing technique is not quantified; however, the effect is expected to worsen as the probe separation increases.

For LR characterization, one eighth of the package was characterized for a total of 26 leads to produce a 26×26 inductance matrix and a 26×1 resistance column. Applying (5) to 26 one-port measurements and (7) to 325 two-port measurements results in the inductance matrix given in Fig. 3. Lead 3 is omitted from the results as there is an obvious problem with the measured result. The measurement for lead 2 also suffers from some problem, but the result is left in. Both leads were probably improperly probed.

The geometry of the package was simulated with a commercial PEEC simulator, where just the leads and wirebonds were included in the simulation. The PEEC method is described in [30]. The ground plane was assumed to be negligible, with zero self- and mutual-inductances and negligible eddy currents, so it is not included in the simulation. In the measurement, the resistance and self-inductance of the leads will dominate that of the ground plane, and the measurement setup minimizes the effects of mutual inductance between the leads and the ground plane by spreading out the current. Therefore, the effects of the ground plane are expected to be negligible in the measurement, allowing the measured and simulated results to be directly compared.

The percent difference between the simulation and measurement at 52.1 MHz is shown in Fig. 4. The simulation was repeated at 4.76 MHz, and the difference is shown in Fig. 5. Both figures show that agreement is very good for the self-inductance terms and for mutual terms for the nearest several leads. Agreement drops off for farther leads, and there is no data to support whether the problem lies with the simulation, measurement, or both. It may be that the ground plane in the measurement enhances the far mutual terms relative to the simulation, which incorporates no ground plane. On the other hand, wide separation of the probes introduces inconsistencies with the reference definition, as discussed earlier, and this inconsistency may be responsible for the disagreement.

Since the technique relies on two-point contacts, contact resistance plays a large role for the small resistances encountered in packaging. The measurement for each lead is uniquely corrupted, but a low-frequency four-probe measurement can

TABLE I
COMPARISON BETWEEN ADJUSTED RESISTANCE MEASUREMENTS AND SIMULATION

Lead and Frequency	Adjusted R, mΩ	Simulation R, mΩ	% Difference
Lead 1 at 4.76 MHz	100	126	-26
Lead 1 at 52.1 MHz	234	171	+27
Lead 26 at 4.75 MHz	126	133	-5.6
Lead 26 at 52.1 MHz	209	166	+21

TABLE II
CAPACITANCE MATRIX MEASUREMENT RESULTS IN pF AT 104 MHz

Lead	24	25	26	27	28
24	0.638	-0.451	-0.043	-0.017	-0.008
25	-0.451	1.070	-0.445	-0.047	-0.014
26	-0.043	-0.445	1.018	-0.375	-0.050
27	-0.017	-0.047	-0.375	1.001	-0.451
28	-0.008	-0.014	-0.050	-0.451	0.638

TABLE III
CAPACITANCE MATRIX SIMULATION RESULTS FROM STATIC FINITE ELEMENT SOLVER

Lead	24	25	26	27	28
24	0.713	-0.551	-0.048	-0.019	-0.010
25	-0.551	1.261	-0.564	-0.045	-0.018
36	-0.048	-0.564	1.211	-0.469	-0.045
27	-0.019	-0.045	-0.469	1.177	-0.560
28	-0.010	-0.018	-0.045	-0.560	0.719

be used to calibrate the high-frequency data. For example, for lead 1, 4-probe measurements yield a resistance of 127 mΩ at 300 kHz, while the network analyzer produced −137 mΩ. The adjustment is then 264 mΩ for all frequencies. The comparison between the corrected measurements and simulation is shown in Table I, where the results for leads 1 and 26 at two frequencies are included. The agreement is moderate and may be considered to be reasonably good for two-point resistance measurements for such small values.

For CG characterization, nine short leads were characterized to produce 9×9 capacitance and conductance matrices. Applying (5) to 9 one-port measurements and (7) to 36 two-port measurements and computing a matrix inversion yields the capacitance and conductance matrices. The matrix inversion is valid for data on a subset of the entire package due to the rapid rolloff of mutual capacitance with distance, a situation which produces a diagonally-dominant matrix. The outer two leads on each side are deleted from the final results since they could be corrupted by the truncation of the matrix. The final 5×5 matrix is shown in Table II, where the results at 104 MHz are shown. Results at other frequencies show all matrix values to be virtually constant with respect to frequency.

The geometry of the same nine leads was simulated with a commercial static finite element simulator. The outer two leads on each side were deleted from the final results since they do not include proper loading by neighboring leads. The results are shown in Table III. The percent difference between the measured and simulated matrices are shown in Table IV. The agreement is acceptable considering how sensitive capacitance is to sample positioning and material dielectric constants. The consistent overestimates produced by the simulation may be due a high value for the dielectric constant of the plastic encapsulant since a nominal value of 3.9 was used in lieu of a measured value. Note that the ground is present and located in the same position in both measurement and simulation so that direct comparison is possible.

TABLE IV
PERCENT DIFFERENCE BETWEEN SIMULATION (TABLE III) AND MEASUREMENT (TABLE II) USING THE MEASURED DATA AS THE BASE

Lead	24	25	26	27	28
24	11.8	22.1	11.0	11.1	28.6
25	22.1	17.9	26.8	-5.7	24.8
26	11.0	26.8	19.0	24.9	-8.8
27	11.1	-5.7	24.9	17.6	24.2
28	28.6	24.8	-8.8	24.2	12.7

The measured conductance matrix is composed of very small values of both positive and negative sign, an indication that the technique cannot resolve the small leakage values seen in good dielectrics.

IV. CONCLUSION

Starting with a lumped-element model, a two-step measurement procedure is outlined that allows the resistance and inductance matrices to be measured on a specially prepared sample. An identical procedure on a separately prepared sample allows the measurement of the conductance and capacitance matrices. The technique is optimized for use with network analyzers.

Measurements and simulations on a 208-lead quad flat pack show that the derived experimental method attains good accuracy in comparison to simulation. For the inductance matrix, agreement is quite good for the self terms and for mutuals to nearby lines. The agreement drops off for widely separated lines, and the lack of agreement may be due to corruption of the reference in the technique used or to the lack of a ground plane in the simulation. For the resistance matrix, contact resistance must be corrected with a 4-probe resistance measurement at a low frequency before the resistance results are useful. Even then, the work here demonstrates only moderate agreement between measurement and simulation for the small resistance values seen. For the capacitance matrix, agreement between simulation and measurement is acceptable for a capacitance measurement, and better agreement may be found should the simulation be repeated with measured values of dielectric constant rather than the nominal values used here. Finally, the conductance matrix consisted of very small values of both positive and negative sign, so the method does not demonstrate utility for conductance measurement on good dielectrics.

REFERENCES

[1] H. Heeb and A. Ruehli, "Three-dimensional interconnect analysis using partial element equivalent circuits," *IEEE Trans. Circuits Syst.-Part I: Fund. Theory Appl.*, pp. 974–982, Nov. 1992.

[2] A. Nakamura *et al.*, "Handling of mutual inductance in simulation of simultaneous switching noise," in *Proc. 44th ECTC*, 1994, pp. 663–668.

[3] L. Yuan and C. Cheng, "Electrical design of a 383PPGA for low voltage swing CMOS transceiver (GTL)," in *Proc. 1993 IEPS*, 1993, pp. 656–662.

[4] E. M. Foster, "The electrical effect of single-chip CMOS packages," *IEEE Trans. Comp., Hybrids, Manufact. Technol.*, pp. 593–603, Dec. 1987.

[5] C. Kryzak, D. Dokos, M. Sanford, and J. Weiss, "Electrical characterization of PGA design for submicron CMOS applications: Simulation and measurement," in *Proc. 1990 IEPS*, 1990, pp. 263–271.
[6] C.-C. Huang and L. L. Wu, "Signal degradation through module pins in VLSI packaging," *IBM J. Res. Develop.*, pp. 489–498, July 1987.
[7] M. Bedouani, "High-density integrated circuit design: Simultaneous switching ground/power noises calculation for pin grid array packages," in *Proc. 43rd ECTC*, 1993, pp. 1039–1044.
[8] A. T. Mu, "Electrical modeling program for high-performance IC packaging—The study of logic circuit behavior (propagation delay, rise time, and fall time) with respect to delta-I noise," in *Proc. 1989 IEPS*, 1989, pp. 359–364.
[9] V. K. Tripathi and N. Orhanovic, "Time-domain characterization and analysis of dispersive dissipative interconnects," *IEEE Trans. Circuits and Systems-Part I: Fund. Theory Appl.*, pp. 938–945, Nov. 1992.
[10] B. J. Cooke, J. L. Prince, and A. C. Cangellaris, "S-parameter analysis of multiconductor, integrated circuit interconnect systems," *IEEE Trans. Computer-Aided Design*, pp. 353–360, Mar. 1992.
[11] A. K. Agrawal, K.-M. Lee, L. D. Scott, and H. M. Howles, "Experimental characterization of multiconductor transmission lines in the frequency domain," *IEEE Trans. Electromagnetic Compat.*, pp. 20–27, Feb. 1979.
[12] V. L. Carey, T. R. Scott, and W. T. Weeks, "Characterization of multiple parallel transmission lines using time domain reflectometry," *IEEE Trans. Instrum. Meas.*, pp. 166–171, Sept. 1969.
[13] A. K. Agrawal, H. M. Fowles, and L. D. Scott, "Experimental characterization of multiconductor transmission lines in inhomogeneous media using time-domain techniques," *IEEE Trans. Electromagnetic Compat.*, pp. 28–32, Feb. 1979.
[14] L. A. Hayden and V. J. Tripathi, "Characterization and modeling of multiple line interconnections from time domain measurements," *IEEE Trans. Microwave Theory Tech.*, pp. 1737–1743, Sept. 1994.
[15] R. E. Canright, "Capacitance: Relationships and measurements," in *Proc. 40th ECTC*, 1990, pp. 163–168.
[16] D. W. Quint, A. Aziz, R. Kaw, and F. J. Perezalonso, "Measurement of R, L, and C parameters in VLSI packages," *Hewlett-Packard J.*, pp. 73–77, Oct. 1990.
[17] A. Deutsch, G. Arjavalingham, G. V. Kopcsay, and M. Degerstrom, "Short-pulse propagation technique for characterizing resistive package interconnection," in *Proc. 42nd ECTC*, 1992, pp. 736–739.
[18] D. E. Carlton, K. R. Gleason, K. Jones, and E. W. Strid, "Accurate measurement of high-speed package and interconnect parasitics," in *Japan IEMT Symp. Digest*, 1989, pp. 276–279.
[19] Y. Takahashi *et al.*, "Ceramic package with 7.6 GHz bandwidth for high-speed LSI chips," *Sumitomo Electric Tech. Rev.*, pp. 256–261, Jan. 1990.
[20] C. J. Stanghan and B. M. MacDonald, "Electrical characterization of packages for high-speed integrated circuits," *IEEE Trans. Comp., Hybrids, Manufact. Technol.*, pp. 468–473, Dec. 1985.
[21] T. S. Tarter and W. Beale, "High frequency package electrical characterization: Meeting the challenge," in *Proc. 1992 IEPS*, 1992, pp. 1164–1185.
[22] L. E. Mosley, D. Mallik, and B. K. Bhattacharyya, "A new technique for measuring the inductance of pin grid array packages," in *Japan IEMT Symp. Digest*, 1989, pp. 280–285.
[23] S. Yamanaka, T. Naida, and T. Ihara, "Electrical properties of aluminum coated fine pitch lead frame for high-pin-count ceramic quad flat package," in *Proc. 1990 ISHM*, 1990, pp. 626–631.
[24] C.-T. Tsai, H. Anderson, and W.-Y. Yip, "Electrical characterization of bonding wires," in *Proc. 1994 ISHM*, 1994, pp. 479–484.
[25] C.-T. Tsai *et al.*, "High-frequency inductance measurements and characterization of Alloy-42 and copper packages," in *Proc. 43rd ECTC*, 1993, pp. 635–640.
[26] C.-T. Tsai, "Package inductance characterization at high frequencies," *IEEE Trans. Comp., Packag., Manufact. Technol.*, pp. 175–181, May 1994.
[27] J. Williams and E. Godshalk, "Characterization and modeling of pin grid array (PGA) packages," in *Proc. 1992 ISHM*, 1992, pp. 623–628.
[28] J. Williams, K. Smith, and E. Godshalk, "Improved techniques for characterization of high-speed packaging," in *Proc. 1991 ISHM*, 1991, pp. 262–266.
[29] Y. Eo and W. R. Eisenstadt, "High-speed VLSI interconnect modeling based on S-parameter measurements," *IEEE Trans. Comp., Hybrids, Manufact. Technol.*, pp. 555–562, Aug. 1993.
[30] A. E. Ruehli, "Inductance calculations in a complex integrated circuit environment," *IBM J. Res. Develop.*, pp. 470–481, Sept. 1972.
[31] S. J. Leon, *Linear Algebra With Applications*. New York: MacMillan, 1980.
[32] JEDEC, "Guidelines for measurement of electronic package inductance and capacitance model parameters," committe ballot JC-15-93-106A, Dec. 28, 1993.

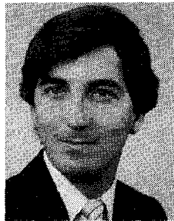

Brian Young received the B.S. degree from Texas A&M University, the M.S. degree from the University of Illinois at Champaign/Urbana, and the Ph.D. degree from the University of Texas at Austin, in 1984, 1985, and 1987, respectively, all in electrical engineering.

He taught electromagnetics at Texas A&M University for three years and researched numerical techniques for waveguide analysis. He worked at Hughes Aircraft Company for two years on microwave packaging and statistical amplifier design. Since 1993, he has been with Motorola in Austin, TX working on measurements and modeling of digital packaging.

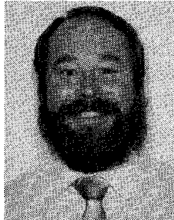

Aubrey K. Sparkman received the B.S.E.E. degree from the University of Texas at Austin, in 1984.

He has worked in the areas of equipment engineering, electrical analysis and design of IC packaging, and wafer probe. He worked at the Microelectronics and Computer Technology Corporation (MCC) in the areas of high density interconnect design and test before moving to Motorola's Semiconductor Products Sector to work on electrical analysis and design of multilayer packaging. He currently leads Motorola's Advanced and Array Probe development for C4 and MCM and is the holder of two Motorola patents in the areas of semiconductor processes and packaging.